

*Tamap Journal of Engineering*



*Volume 2017, Article ID 4*

*Research Article*

## COMPUTATIONAL INVESTIGATION OF SELF PROPULSION PERFORMANCE OF DARPA SUBOFF VEHICLE

Cihad Delen<sup>1</sup>, Savas Sezen<sup>2</sup>, Sakir Bal<sup>1\*</sup>

<sup>1</sup> Istanbul Technical University, Faculty of Naval Architecture and Ocean Engineering

<sup>2</sup> Yildiz Technical University, Faculty of Naval Architecture and Maritime

\* Corresponding author, e-mail: (sbal@itu.edu.tr)

*Received: 03 March 2017 / Accepted: 31 March 2017*

---

**Abstract:** In this paper, the resistance and power values which are very important for the hydrodynamic performance of an underwater vehicle (DARPA SUBOFF) have been calculated using both an empirical method and Computational Fluid Dynamics (CFD) analysis. The self-propulsion of the vehicle has been investigated using Actuator Disc Theory (ADT). The open water hydrodynamic characteristics of DTMB 4119 propeller that is selected for CFD validation has been merged into ADT. In CFD analyses, the flow around DARPA SUBOFF has been solved using Reynolds Averaged Navier-Stokes (RANS) equations by finite volume method (FVM). During all analyses, the flow has been considered as 3-D, turbulent, incompressible and steady. The numerical results have been compared with the experiments. The self-propulsion performance of DARPA SUBOFF has been computed for two different velocities.

**Keywords:** Actuator Disc Theory, CFD, DARPA SUBOFF, DTMB4119, Hydrodynamic Design, Resistance, Self-Propulsion

---

## INTRODUCTION

The autonomous underwater vehicles (AUV) have become widespread in recent years. The design of AUVs, which are generally used for military and research purposes, is a very difficult task. The variability of working conditions and the difficulty of the mission to be accomplished are very important in the design stage of the vehicle. Therefore, the main issues such as hydrodynamic performance (resistance and propulsion factors) should be determined precisely and reliably in the design stage of AUVs. In this study, the hydrodynamic performance factors (such as resistance and propulsion) of the DARPA AUV form, which is used frequently for validation, have been investigated by CFD analysis.

In the past, the propulsion performance of the appended DARPA SUBOFF vehicle with E1619 model propeller has been studied in [1]. The effect of different bow and stern geometries of bared DARPA form on resistance have been investigated by CFD in [2]. The interaction between propeller and submarine hull has been analyzed with the effects of free surface in [3]. The results showed a good agreement with the experiments. The flow around the DARPA

SUBOFF bare hull with the help of both RANS (Reynolds Averaged Navier-Stokes) and DNS (Direct Numerical Simulation) has been solved in [4], and the pressure and frictional resistance components have been computed in [4]. In [5], the resistance values of submerged form at various velocities using model tests have been compared with those of CFD and empirical methods. The resistance and propulsion analyses of an AUV have been performed in [6]. The actuator disc theory has been used in the self-propulsion analysis. The propeller-ship interaction has been investigated by a commercial CFD program for DTC Post-Panamax Container Ship in [7]. The ship has been analyzed without taking free surface effects into account.

In this study, the hydrodynamic characteristics (such as resistance, propulsion, and wake values) of the DARPA bare hull form have been investigated by CFD based method. DTMB4119 model propeller, which is frequently used for validation, has been used to determine the self-propulsion prediction of AUV. The resistance values of vehicle obtained by solving the flow around the underwater vehicle are first compared with the experimental results. Later, the flow around the DTMB4119 model propeller has been solved by CFD and the obtained results have been compared with the experimental open water results. Finally, the propulsion performance of DARPA AUV has been estimated by using actuator disc which has the same main dimensions and hydrodynamic factors with DTMB 4119 propeller. The propeller hull interaction has also been investigated using Actuator Disc Theory.

## MATHEMATICAL MODEL AND METHODS

### RANS Method

The governing equations are the continuity equation and the well-known RANS equations for the unsteady, three-dimensional and incompressible flow [8]. The continuity can be given as;

$$\frac{\partial U_i}{\partial x_i} = 0 \quad (1)$$

While the momentum equations are expressed as,

$$\frac{\partial U}{\partial t} + \frac{\partial (U_i U_j)}{\partial x_j} = -\frac{1}{\rho} \frac{\partial P}{\partial x_i} + \frac{\partial}{\partial x_j} \left[ \nu \left( \frac{\partial U_i}{\partial x_j} + \frac{\partial U_j}{\partial x_i} \right) \right] - \frac{\partial \overline{u_i' u_j'}}{\partial x_j} \quad (2)$$

All analyses are carried out for steady state case, so the first term in Eq. (2) is not taken into account. In momentum equations,  $U_i$  and  $u_i'$  represent the mean velocity and the fluctuation velocity components in the direction of the Cartesian coordinate  $x_i$ , respectively.  $P$ ,  $\rho$  and  $\nu$  express the mean pressure, the density and the kinematic viscosity coefficient, respectively.

The k- $\varepsilon$  turbulence model is employed in order to simulate the turbulent flow around the AUV precisely. This turbulence model is applicable when there are not high pressure changes along the form and separation near the vehicle. The k- $\varepsilon$  turbulence model is used because the vessel is submerged and there are no free surface effects. During the analyses, Reynolds stress tensor is also calculated as follow,

$$\overline{u_i' u_j'} = -\nu_t \left( \frac{\partial U_i}{\partial x_j} + \frac{\partial U_j}{\partial x_i} \right) + \frac{2}{3} \delta_{ij} k \quad (3)$$

Here,  $\nu_t$  is the eddy viscosity and can be expressed as  $\nu_t = C_\mu k^2 / \varepsilon$  while  $C_\mu$  is an empirical constant ( $C_\mu = 0.09$ ). The  $k$  is the turbulent kinetic energy and  $\varepsilon$  is the turbulent dissipation rate. In addition to the continuity and momentum equations, two transport equations are solved for  $k$  and  $\varepsilon$ :

$$\frac{\partial k}{\partial t} + \frac{\partial(kU_j)}{\partial x_j} = \frac{\partial}{\partial x_j} \left[ \left( v + \frac{v_t}{\sigma_k} \right) \frac{\partial k}{\partial x_j} \right] + P_k - \varepsilon \quad (4)$$

$$\frac{\partial k}{\partial t} + \frac{\partial(kU_j)}{\partial x_j} = \frac{\partial}{\partial x_j} \left[ \left( v + \frac{v_t}{\sigma_k} \right) \frac{\partial k}{\partial x_j} \right] + P_k - \varepsilon \quad (5)$$

$$\frac{\partial \varepsilon}{\partial t} + \frac{\partial(kU_j)}{\partial x_j} = \frac{\partial}{\partial x_j} \left[ \left( v + \frac{v_t}{\sigma_\varepsilon} \right) \frac{\partial \varepsilon}{\partial x_j} \right] + C_{\varepsilon 1} P_k \frac{\varepsilon}{k} - C_{\varepsilon 2} \frac{\varepsilon^2}{k} \quad (6)$$

$$P_k = -\overline{u_i' u_j'} \frac{\partial U_i}{\partial x_j} \quad (7)$$

where,  $C_{\varepsilon 1} = 1.44$   $C_{\varepsilon 2} = 1.92$ , turbulent Prandtl numbers for  $k$  and  $\varepsilon$  are  $\sigma_k = 1$  and  $\sigma_\varepsilon = 1$ , respectively[9]. Further explanations for the  $k$ - $\varepsilon$  turbulence model can be found in [10].

### Actuator Disc Theory

In actuator disc theory, an infinitely thin disc having the same diameter with the real propeller is taken into consideration and the momentum change of the fluid passing through this disc is investigated [11-13]. Some assumptions in this theory are as follows;

- The fluid passing through disc gains energy and this energy (thrust, velocity) is the same at each point of disc.
- The flow is steady, incompressible, irrotational and inviscid.
- There is no tangential velocity and there are only radial and axial velocities.

Also the classical Rankine-Froude theory considers the balance of axial-momentum far up and downstream the system for a uniformly loaded actuator disc without rotation [14]. As shown in Fig. 1, the flow moves from the left to the right. The locations where the velocities are  $V_A$  and  $V_C$ , represent freestream and the slipstream of the actuator disc, respectively. The location shown by  $V_B$  is the actuator disc area.

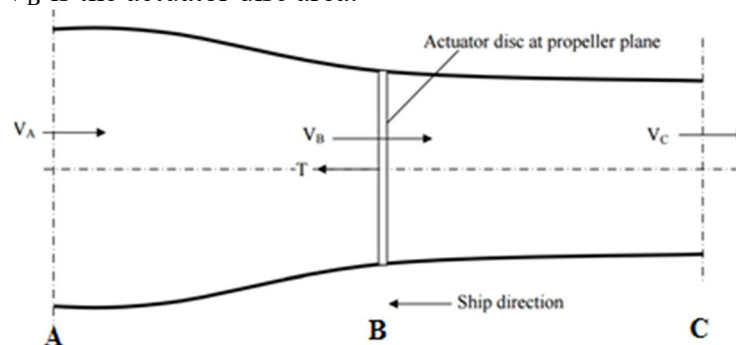


**Figure 1.** Flow field around the actuator disc [15].

The force ( $T$ ), on the disc is

$$T = \dot{m}(V_C - V_A) \quad (8)$$

Here, the mass flow ( $\dot{m}$ ) through the disc is given as  $\dot{m} = \rho V_B A$ , where  $A$  is the disc area of section,  $\rho$  is the density. The velocity at the disc ( $V_B$ ) can be found the arithmetic mean of  $V_A$  and the  $V_C$  by applying Bernoulli equation in the regions  $A$  and  $C$ , then it can be express as follow in terms of the  $V_A$  and  $V_C$ ,

$$V_B = \frac{1}{2}(V_C + V_A) \quad (9)$$

$$V_B = V_A + u_a \quad (10)$$

$$V_C = V_A + u_{a1} \quad (11)$$

Here,  $u_a$  and  $u_{a1}$  are the induced velocities.  $V_B$  cannot be measured or calculated directly [15]. The velocities can then be obtained using mass conservation through the disc gives that  $A_A V_A = A_B V_B = A_C V_C$ . Eventually,  $T$  is determined as,

$$T = \frac{\pi}{4} D^2 \rho (V_A + u_a) u_{a1} \quad (12)$$

The detailed information about theory is given in [14-16].

### Empirical Approach

In this study, an empirical formula developed before for the submarines has been investigated in [5]. Four empirical approaches have been investigated in their work and compared with the results of experiments and CFD. The second method mentioned in the study was found to have the closest results to the experiments and CFD analysis and it has then been selected to apply to DARPA SUBOFF in this study. This method is briefly described as below [5].

The additional resistance coefficient from the roughness is taken as 5% of the frictional coefficient ( $C_{F0}$ ) value calculated according to the ITTC 1957 [17]. This coefficient is summed with  $C_{F0}$  and the new  $C_F$  value is calculated as follows.

$$C_{F0} = \frac{0.075}{(\log Re - 2)^2} \quad (13)$$

$$\delta C_F = 0.05 C_{F0} \quad (14)$$

$$C_F = C_{F0} + \delta C_F \quad (15)$$

The form factor ( $k$ ) is calculated by Eq. 16. The  $k$  value is multiplied by  $C_{F0}$  to obtain the viscous pressure coefficient ( $C_{VP}$ ). The total resistance coefficient ( $C_T$ ) could be obtained by summing the  $C_F$  and  $C_{VP}$  coefficients for submerged bodies. Then the resistance value ( $R_T$ ) is obtained from Eq. 19,

$$k = \frac{D}{L} + 1.5 \left( \frac{D}{L} \right)^3 \quad (16)$$

$$C_{VP} = C_{Form} = k \cdot C_{F0} \quad (17)$$

$$C_T = C_F + C_{VP} \quad (18)$$

$$R_T = 0.5 C_T \rho S V^2 \quad (19)$$

where  $D$  is the maximum diameter of the form and  $L$  is the length of the form,  $\rho$  is the density of fluid,  $V$  is the velocity and  $S$  is the wetted surface area.

Actually the forces on submerged body are the frictional and viscous forces. Since DARPA SUBOFF has almost a slender hull form, empirical methods could be used to determine these forces during the preliminary design stage.

## RESULTS AND DISCUSSION

### Open Water Results of DTMB4119 Model Propeller

First, the open water hydrodynamic performance of the DTMB4119 model propeller used in the propulsion analysis has been analyzed by CFD in a wide range of advance coefficients ( $J$ ). The open water computations were carried out as steady flow using  $k-\epsilon$  turbulence model with the aid of a Moving Reference Plane (MRF). The main properties and three-dimensional view of the DTMB4119 model propeller are given in Table 1 and Fig.2. The open water results calculated by CFD analysis have been compared with the experiments in Fig. 3. The differences

in dimensionless thrust and torque coefficients are approximately 1%-2%. The open water calculations of the DTMB4119 model propeller by CFD have been shown in detail in [18].

Table 1. The main features of DTMB4119 Model Propeller.

Delivered power ( $P_D$ ) (kW)	0.474
Advance velocity ( $V_A$ ) (m/s)	2.54
Diameter (D) (m)	0.3048
Rate of Revolution (rps)	10
Skew ( $^\circ$ )	0
Rake ( $^\circ$ )	0
Blade section	NACA66 a=0.8
Number of blades (Z)	3

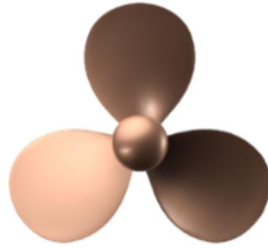


Figure 2. DTMB4119 Model Propeller.

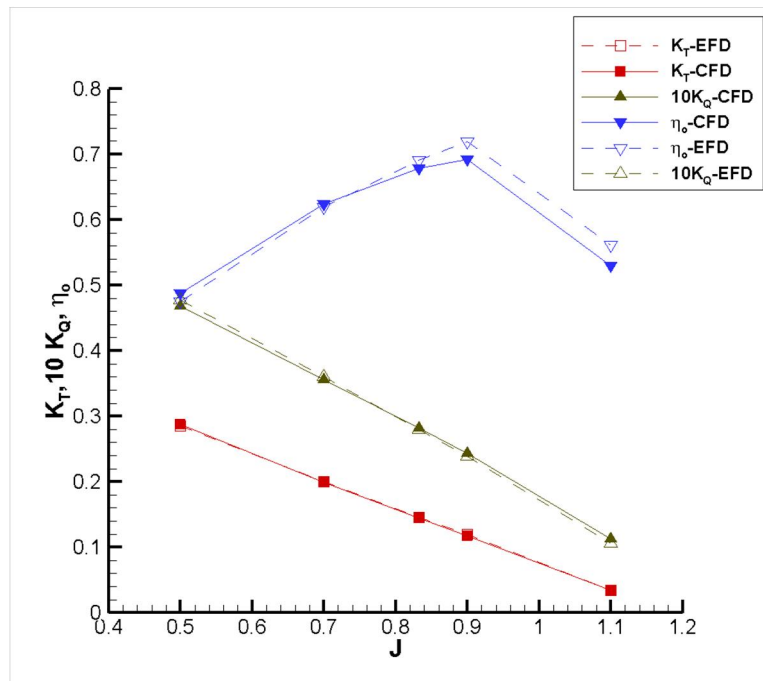


Figure 3. Open water performance characteristics of DTMB 4119.

### Resistance Computation of DARPA SUBOFF by CFD and Empirical Methods

The DARPA SUBOFF form is an underwater vehicle that is often used for validation. The bare configuration of the model is known as AFF-1 [19]. There is no appendage (sail, rudder, fin, etc.) on this form [20]. In this study, only the AFF-1 form that is bare vehicle has been analyzed. The main properties and three-dimensional view of the DARPA SUBOFF form are given in Table 2 and Fig. 4.

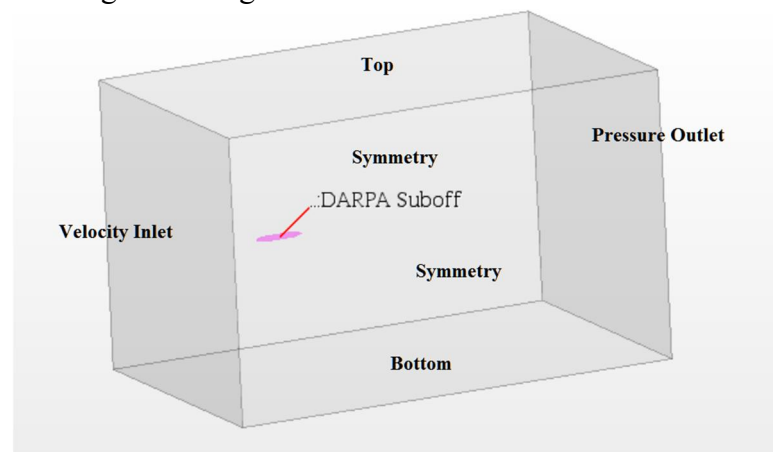
Table 2. The main properties of the DARPA SUBOFF form.

Length between perpendiculars ( $L_{BP}$ ) (m)	4.261
Length overall ( $L_{OA}$ ) (m)	4.356
Maximum hull radius ( $R_{MAX}$ ) (m)	0.254
Wetted surface area (S) ( $m^2$ )	5.988
Displacement volume ( $\nabla$ ) ( $m^3$ )	0.699



Figure 4. A view of DARPA SUBOFF bare form.

The initial and boundary conditions in CFD analyses must be carefully determined depending on the flow problem. Appropriate boundary conditions can also reduce the cost of calculations [21]. Because of the axial symmetry of the submerged form, analysis can be carried out by creating computational domain longitudinally half or quarter of the form to simplify the problem and reduce the time of the analysis. This type of application has generally advantageous for the resistance analysis. But, the full model must be used in order to accurately reflect the propeller effect in the propulsion performance of the form. The main dimensions of the computational domain are determined in accordance with the ITTC guidelines [22]. The main dimensions of the computational domain have been determined as  $9L$  length,  $8L$  width,  $8L$  height so as not to be affected by free water surface and wall effects, respectively. A 3-D view of the computational domain is given in Fig. 5.



.Figure 5. A view of computational domain.

As shown in Fig. 5, the left side of the computational domain is defined as velocity inlet and the right side is defined as pressure outlet. In addition, the side surfaces are also defined as symmetry.

The computational domain is divided into three dimensional finite volumes and discretized according to the finite volume method (FVM). To create a computational domain, unstructured hexahedral elements are employed in the whole domain. The mesh refinements are also made in the bow, stern and the wake area of the form. Unstructured mesh of the computational domain is given in Fig. 6. In CFD analyses, optimum cell number has been determined with verification and validation study. Total cell number is about 1.2 million.

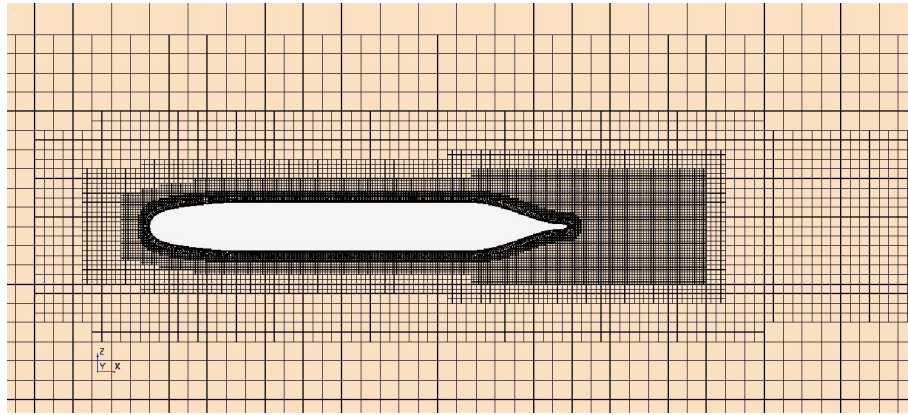


Figure 6. Unstructured mesh of the computational domain.

The resistance analysis of the DARPA SUBOFF has been computed by CFD analysis and empirical approach for different speeds. The  $k-\varepsilon$  turbulence model has been used and the flow analyses have been carried out as steady.

The numerical results ( $R_{T-CFD}$ ) are in good agreement with the experimental ones ( $R_{T-EXP}$ ) as can be seen in Table 3. The maximum relative error between the CFD and experimental results is 0.7%. On the other hand, the relative error between the experiments and the resistance values obtained by the empirical approach ( $R_{T-EMP}$ ) is higher than those of CFD analyses. This may be due to the empirical method used for computation of form factor.

Table 3. The resistance values of DARPA SUBOFF bare form.

V (m/sn)	$R_{T-EXP}$ (N)	$R_{T-CFD}$ (N)	Relative error of CFD (%)	$R_{T-EMP}$ (N)	Relative error of EMP (%)
3.046	87.4	87.32	0.1	94.65	8.3
5.144	242.2	241.18	0.4	247.33	2.1
6.091	332.9	330.96	0.6	337.31	1.3
7.161	451.5	449.46	0.5	454.26	0.6
8.231	576.9	572.66	0.7	587.03	1.8
9.255	697	696.15	0.1	728.58	4.5

#### Self-Propulsion Points of DARPA SUBOFF by Actuator Disc Theory

The DARPA bare form has been later analyzed for self-propulsion. For the propulsion performance test, a disc has been defined on the propeller plane of the DARPA form (where  $x/L = 0.987$ ) by Actuator Disc Theory. The diameter and thickness of the disc have been taken as similar to DTMB 4119 model propeller. In Fig. 7, DTMB4119 propeller and the disc according to the specified specifications are shown together.



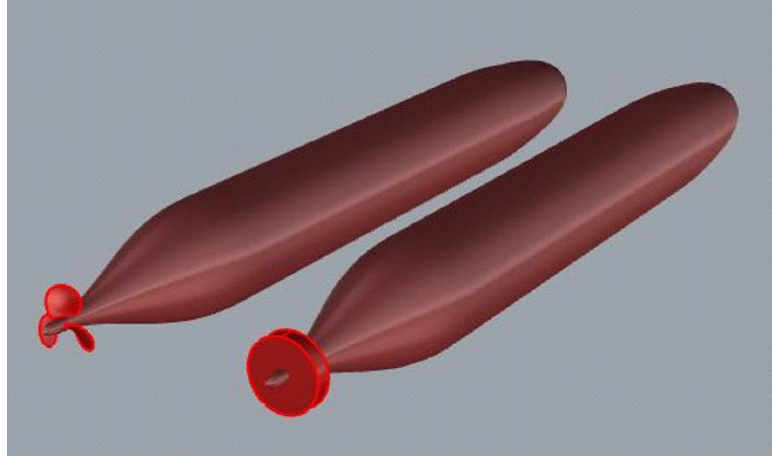


Figure 7. The propeller and the virtual disc behind the submarine.

Open water results of the DTMB 4119 have been used in the self-propulsion analyses. In this study, the self-propulsion points have been investigated at 3.046 m/s and 5.144 m/s. The distributions of the axial velocity are shown in Fig. 8 and 9 for two different flow velocities, respectively. The stream lines around the actuator disc and DARPA SUBOFF are presented in Fig. 10 for 3.046 m/s.

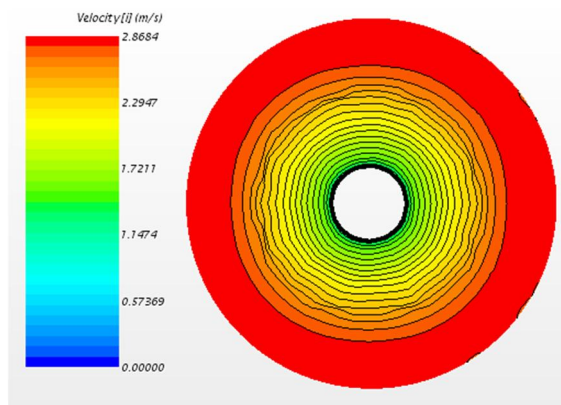


Figure 8. The axial velocity distributions on the propeller plane ( $V=3.046$  m/s)

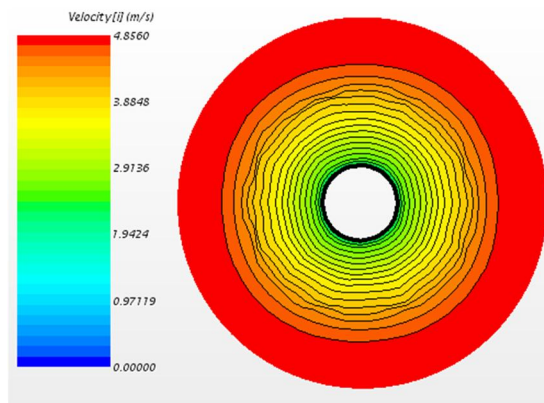


Figure 9. The axial velocity distributions on the propeller plane ( $V=5.144$  m/s)



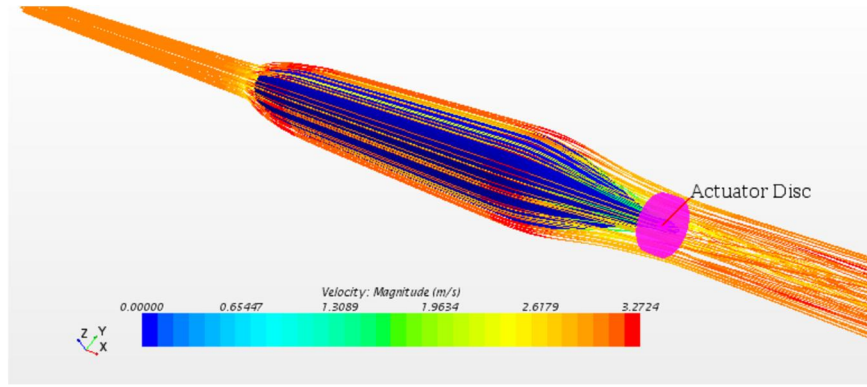


Figure 10. The stream lines around the DARPA SUBOFF at  $V=3.046$  m/s.

The non-dimensional pressure coefficient has been calculated as below;

$$C_p = \frac{P}{1/2\rho V_s^2} \quad (20)$$

Here,  $P$  is the dynamic pressure acting on the submarine bare hull form. The non-dimensional pressure distributions on the hull surface have been given in Fig. 11 for  $V=3.046$  m/s and  $V=5.144$  m/s, respectively.

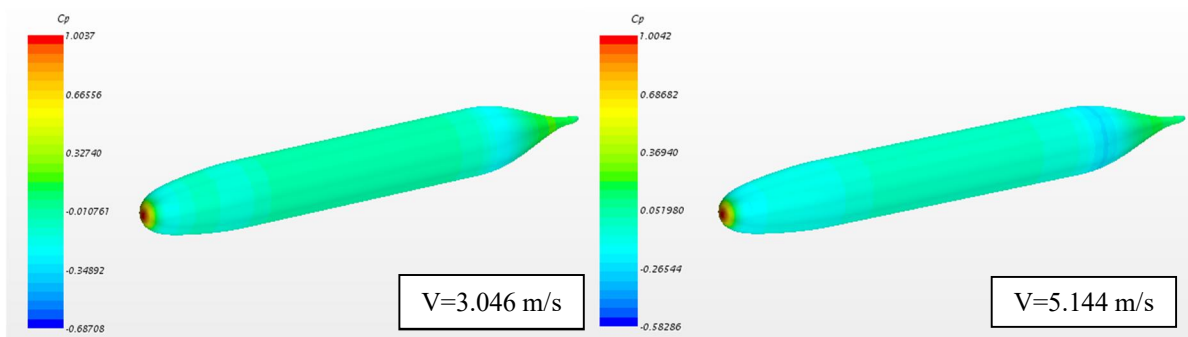


Figure 11. The non-dimensional pressure distributions on the hull surface.

The change in thrust and resistance of the submarine with virtual disc versus the propeller rate of revolution are shown in Fig. 12 and 13 for the velocities of 3.046 m/s and 5.144 m/s, respectively. It is clear from the figures that small changes in the disc rotational speed rapidly cause a change in the thrust values. Self-propulsion points for both velocities have been determined by considering that the self-propulsion is the point where the submarine resistance is equal to the thrust generated by the virtual disc. Self-propulsion points for velocities of 3.046 m/s and 5.144 m/s are found as 9.824 rps and 16.457 rps, respectively.

The required engine power for these velocities have also been calculated from thrust and torque values and the ITTC self-propulsion procedure for these rotational speeds [23]. The self-propulsion characteristics of the DARPA SUBOFF for the velocities of 3.046 m/s and 5.144 m/s are given in Table 5. The methodology followed here for performance propulsion of a hull is briefly described as follows [23]:

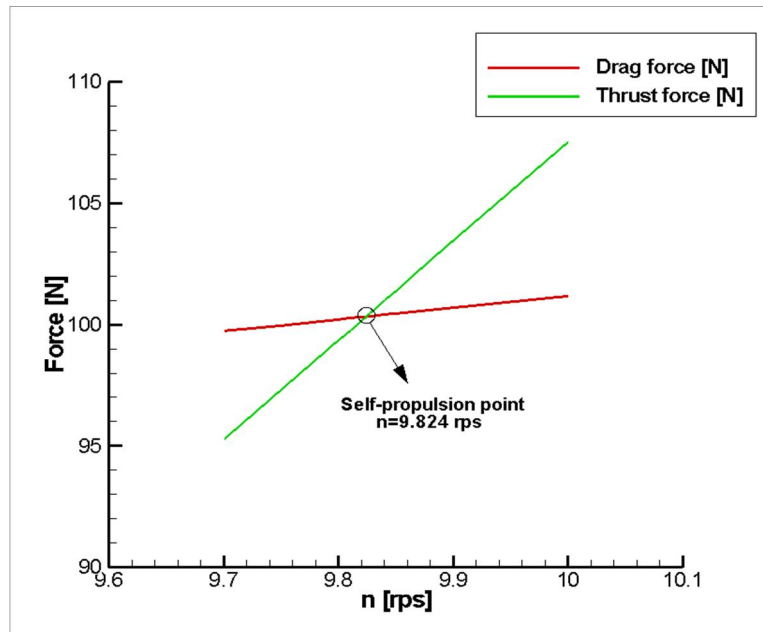


Figure 12. Self-propulsion point for  $V=3.046$  m/s.

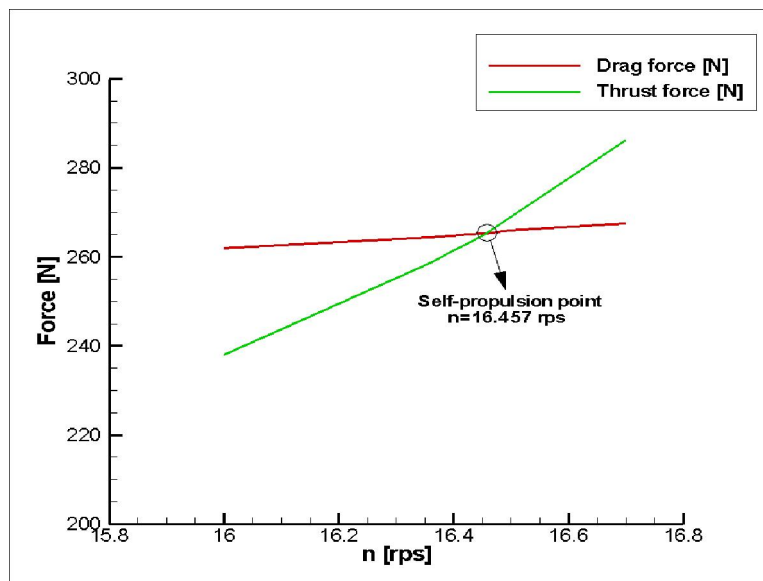


Figure 13. Self-propulsion point for  $V=5.144$  m/s.

The effective wake coefficient here is calculated as follow; (21)

$$w=1-V_A/V_S$$

Here,  $V_A$  is the average flow velocity in the propeller (disc) plane,  $V_S$  is the incoming flow velocity towards the hull.  $V_A$  is calculated by

$$V_A=JnD \quad (22)$$

where  $J$  is advance ratio.  $t$  is the thrust deduction factor that can be calculated by

$$t=1-R_T/T \quad (23)$$

where  $T$  is thrust. The hull efficiency ( $\eta_H$ ) is expressed as the ratio of effective power to propeller thrust power. In another words, it is expressed as follows,

$$\eta_H=(1-t)/(1-w) \quad (24)$$

The relative rotation efficiency ( $\eta_R$ ) is expressed as the ratio of the open water torque value ( $Q_0$ ) of the propeller at the same revolution speed and the speed, to the torque value ( $Q$ ) working behind the vehicle.

$$\eta_R = Q_0/Q \quad (25)$$

The efficiency of the open-water propeller ( $\eta_o$ ) at  $V_A$  is calculated with the help of the following equation.

$$\eta_o = TV_A / 2\pi n Q_0 \quad (26)$$

The self-propulsion efficiency ( $\eta_D$ ) is expressed as follow,

$$\eta_D = \eta_H \eta_o \eta_R \quad (27)$$

Effective power ( $P_E$ ) is the power value required to pull the form at constant speed ( $V_S$ ).

$$P_E = R_T V_S \quad (28)$$

The power delivered to the propeller ( $P_D$ ) is calculated as follow,

$$P_D = P_E / \eta_D \quad (29)$$

Table 5. The self-propulsion characteristics of DARPA Suboff Form.

	$V_s$ (m/s)	$V_s$ (m/s)		$V_s$ (m/s)	$V_s$ (m/s)
	3.046	5.144		3.046	5.144
$V_A$ (m/s)	2.70	4.588	t	0.13	0.087
J	0.903	0.915	$\eta_H$	0.98	1.024
n (rps)	9.824	16.457	$\eta_R$	1.02	1.04
$R_{T-Bare Form}$ (N)	87.4	242.2	$\eta_o$	0.70	0.68
$R_{T-Actuator Disc}$ (N)	100.325	265.21	$\eta_D$	0.69	0.72
T (N)	100.325	265.21	$P_E$ (W)	266.1	1245.9
Q (N.m)	6.107	16.298	$P_D$ (W)	376.9	1685.3
$W_{effective}$	0.112	0.108			

## CONCLUSIONS

In this study, resistance values of DARPA SUBOFF have been computed by both CFD and empirical approaches for different velocities. The open water analyses of DTMB 4119 propeller have been carried out numerically and the results have been validated with available experimental data. Both resistance values of DARPA SUBOFF and open water results of DTMB 4119 propeller have been found to be in good agreement with the experiments given in the literature. Later, the self-propulsion characteristics of DARPA SUBOFF have been determined for  $V=3.046$  m/s and  $V=5.144$  m/s. It should be mentioned that the method is ideal due to ignoring the losses and the computed power is minimum. It is found that applying the actuator disc theory in self-propulsion tests with CFD is robust in terms of computational cost and time. Thus, the self-propulsion characteristics of an underwater vehicle can be found easily by the actuator disc model.

## ACKNOWLEDGEMENTS

The authors would like to thank Asst. Prof. Ali Dogrul from Yildiz Technical University for his valuable support.

## REFERENCES

- [1] N. Chase and P. M. Carrica, "Submarine propeller computations and application to self-propulsion of DARPA Suboff," *Ocean Eng.*, **2013**, 60, pp. 68–80.
- [2] G. Budak and S. Beji, "Computational Resistance Analyses of a Generic Submarine Hull Form and Its Geometric Variants", *J. Ocean Technology*, **2016**, 11, pp. 77-86.

- [3] N. Zhang and S. Zhang, “Numerical simulation of hull/propeller interaction of submarine in submergence and near surface conditions,” *J. Hydrodyn. Ser B*, **2014**, 26, pp. 50–56.
- [4] A. Gross, A. Kremheller, A. Kremheller and H.F. Fasel, “Simulation of Flow over Suboff Bare Hull Model”, AIAA Aerospace Sciences Meeting, **2011**, Orlando, Florida.
- [5] M. Moonesun, M. Javadi, P. Charmdooz and K. U. Mikhailovich, “Evaluation of submarine model test in towing tank and comparison with CFD and experimental formulas for fully submerged resistance”, *Indian J. Geo-Mar. Sci.*, **2013**, 42, pp. 1049–1056.
- [6] C. Delen, S. Sezen and S. Bal, “Numerical Investigation of the Self-Propulsion Performance of an Underwater Vehicle,” The 1<sup>st</sup> International Shipbuilding and Marine Technology Congress (GMO-Shipmar 2016), **2016**, Istanbul, Turkey (In Turkish).
- [7] O.K. Kinaci, A. Kukner and Bal, S. “On propeller performance of DTC Post Panamax container ship” *International Journal of Ocean System Engineering*, **2013**, 3(2), pp. 77-89.
- [8] Y. Cengel and J. M. Cimbalk, “Essentials of fluid mechanics: fundamentals and applications”, **2008**, McGraw-Hill Higher Education.
- [9] D. C. Wilcox, “Formulation of the k-w Turbulence Model Revisited,” *AIAA J.*, **2008**, 46, 11, pp. 2823–2838.
- [10] D. C. Wilcox, “Turbulence modeling for CFD”, DCW Industries Inc., La Canada, California, USA, **1993**.
- [11] M. O. L. Hansen, *Aerodynamics of wind turbines: rotors, loads and structure*, James & James, London, UK, **2003**.
- [12] T. Burton, Ed., “Wind Energy Handbook”, 2<sup>nd</sup> Edn., J. Wiley, UK, **2011**.
- [13] G.T. Houlsby, S. Draper, and M.L.G. Oldfield, “Application of Linear Momentum Actuator Disc Theory to Open Channel Flow,” University of Oxford, Department of Engineering Science, **2008**, OUEL 2296/08.
- [14] R. Mikkelsen, “Actuator disc methods applied to wind turbines”, Technical University of Denmark, F. M. Department of Mechanical Engineering, and MEK, Lyngby, **2003**.
- [15] Z.S. Spakovszky, “Thermodynamics and Propulsion Lecture Notes”, Massachusetts Institute of Technology (MIT), **2006**, Ch. 11-7.
- [16] J. E. Kerwin, J. B. Hadler, and J. R. Paulling, “Propulsion”, Jersey City, N.J: Society of Naval Architects and Marine Engineers, **2010**.
- [17] ITTC, “Report of Resistance Committee”, Proceedings of 8<sup>th</sup> ITTC, **1957**, Madrid, Spain.
- [18] S. Sezen S., A. Dogrul and S. Bal, “Investigation of Marine Propeller Noise for Steady and Transient Flow,” The 1<sup>st</sup> International Shipbuilding and Marine Technology Congress (GMO-Shipmar 2016), **2016**, Istanbul, Turkey.
- [19] H. L. Liu and T. T. Huang, “Summary of DARPA SUBOFF experimental program data”, **1998**, CRDKNSWC/HD-1298-11.
- [20] N.C. Groves, T.T. Huang, and M.S. Chang, “Geometric characteristics of DARPA SUBOFF models (DTRC Model Nos. 5470 and 5471)”, **1989**, DTRC/SHD-1298-01.
- [21] A. Dogrul, “Experimental and numerical investigation of ship resistance and free surface deformations,” *PhD Thesis*, **2015**, Yildiz Technical University, (In Turkish).
- [22] ITTC, “Practical guidelines for ship CFD applications,” Proceedings of 26<sup>th</sup> ITTC, **2011**, Rio de Janeiro.
- [23] ITTC, “Report of Performance Committee,” Proceedings of 15<sup>th</sup> ITTC, Hague, **1978**.